

# Fermi-Pasta-Ulam model with long-range interactions: Dynamics and thermostatics

H. CHRISTODOULIDI<sup>1</sup>, C. TSALLIS<sup>2,3</sup> and T. BOUNTIS<sup>1</sup>

<sup>1</sup> Center for Research and Applications of Nonlinear Systems (CRANS), Department of Mathematics, University of Patras - GR-26500, Patras, Greece

<sup>2</sup> Centro Brasileiro de Pesquisas Físicas and National Institute of Science and Technology for Complex Systems Rua Xavier Sigaud 150, 22290-180 Rio de Janeiro-RJ, Brazil

<sup>3</sup> Santa Fe Institute - 1399 Hyde Park Road, Santa Fe, NM 87501, USA

received 29 May 2014; accepted in final form 2 November 2014

published online 20 November 2014

PACS 05.20.-y – Classical statistical mechanics

PACS 05.45.-a – Nonlinear dynamics and chaos

PACS 65.40.gd – Entropy

**Abstract** – We study a long-range-interaction generalisation of the one-dimensional Fermi-Pasta-Ulam (FPU)  $\beta$ -model, by introducing a quartic interaction coupling constant that decays as  $1/r^\alpha$  ( $\alpha \geq 0$ ) (with strength characterised by  $b > 0$ ). In the  $\alpha \rightarrow \infty$  limit we recover the original FPU model. Through molecular dynamics we show that i) for  $\alpha \geq 1$  the maximal Lyapunov exponent remains finite and positive for an increasing number of oscillators  $N$ , whereas, for  $0 \leq \alpha < 1$ , it asymptotically decreases as  $N^{-\kappa(\alpha)}$ ; ii) the distribution of time-averaged velocities is Maxwellian for  $\alpha$  large enough, whereas it is well approached by a  $q$ -Gaussian, with the index  $q(\alpha)$  monotonically decreasing from about 1.5 to 1 (Gaussian) when  $\alpha$  increases from zero to close to one. For  $\alpha$  small enough, a crossover occurs at time  $t_c$  from  $q$ -statistics to Boltzmann-Gibbs (BG) thermostatics, which defines a “phase diagram” for the system with a linear boundary of the form  $1/N \propto b^\delta/t_c^\gamma$  with  $\gamma > 0$  and  $\delta > 0$ , in such a way that the  $q = 1$  (BG) behaviour dominates in the  $\lim_{N \rightarrow \infty} \lim_{t \rightarrow \infty}$  ordering, while in the  $\lim_{t \rightarrow \infty} \lim_{N \rightarrow \infty}$  ordering  $q > 1$  statistics prevails.

Copyright © EPLA, 2014

More than one century ago, in his historical book *Elementary Principles in Statistical Mechanics* [1], Gibbs remarked that systems involving long-range interactions will be intractable within his and Boltzmann’s theory, due to the divergence of the partition function. This is of course the reason why no standard temperature-dependent thermostatical quantities (*e.g.*, specific heat) can possibly be calculated for the free hydrogen atom, for instance. Indeed, unless a box surrounds the atom, an infinite number of excited energy levels accumulate at the ionisation value, which yields a divergent canonical partition function at any finite temperature. Related discussions can be seen in [2–5], for instance.

To investigate the deep consequences of Gibbs’ remark, we focus on the influence of the linear and nonlinear long-range interactions (LRI) within an isolated system. In particular, we use the classical Fermi-Pasta-Ulam (FPU)  $\beta$ -model [6–10], which combines linear and nonlinear nearest-neighbor interactions and allows to study

separately the linear and nonlinear nature of the LRI. In the present paper we focus primarily on the FPU  $\beta$ -model with nonlinear LRI, since the most interesting phenomena appear in this case, although we write the Hamiltonian in a compact form which includes both kinds of long range:

$$\mathcal{H} = \frac{1}{2} \sum_{n=1}^N p_n^2 + \frac{1}{2\tilde{N}_{lin}} \sum_{n=0}^N \sum_{m=n+1}^{N+1} \frac{(x_n - x_m)^2}{(m-n)^{\alpha_{lin}}} + \frac{b}{4\tilde{N}} \sum_{n=0}^N \sum_{m=n+1}^{N+1} \frac{(x_n - x_m)^4}{(m-n)^\alpha} \quad (b > 0; \alpha, \alpha_{lin} \geq 0). \quad (1)$$

Fixed boundary conditions (FBC) have been considered, *i.e.*,  $x_0 = x_{N+1} = p_0 = p_{N+1} = 0$ , unit masses without loss of generality, and unit nearest-neighbor coupling constant;  $p_n$  and  $x_n$  are canonical conjugate pairs. At the fundamental state, all oscillators are still at  $x_n = 0$ . The nonlinear part of the potential energy *per particle* varies

with  $N$  like

$$\tilde{N}(N, \alpha) \equiv \frac{1}{N} \sum_{i=0}^N \sum_{j=i+1}^{N+1} \frac{1}{(j-i)^\alpha} = \frac{1}{N} \sum_{i=0}^N \frac{N+1-i}{(i+1)^\alpha} \quad (2)$$

and the linear one like  $\tilde{N}_{lin} \equiv \tilde{N}(N, \alpha_{lin})$ . We notice that  $\tilde{N}(N, 0) \simeq N/2$ , and  $\tilde{N}(\infty, \alpha) = \zeta(\alpha)$ , where  $\zeta(\alpha)$  is the Riemann zeta function. Let us remark that the  $\tilde{N}$  scaling is introduced in the Hamiltonian so as to make (following the current use) the total energy  $U(N)$  (both kinetic and potential contributions) *extensive* (*i.e.*, proportional to  $N$ ) for all values of  $\alpha$ . We note that the above scaling  $\tilde{N}(N, \alpha)$  applies to lattices with fixed boundary conditions and is only slightly different from the analogous scaling found in [11,12] used for periodic boundary conditions (PBC).

The two limits i)  $\alpha \rightarrow 0$  and ii)  $\alpha \rightarrow \infty$  are particularly interesting since they correspond to the extremal cases where i) each particle interacts equally with all others independently of the distance between them and ii) only interactions with nearest neighbors apply, recovering exactly the Hamiltonian of the FPU  $\beta$ -model.

We note here that a significant difference of the present study from the generalised mean-field Hamiltonian (HMF) model [11–13] lies in the implementation of LRI *only in the quartic* part of the potential in (1) (the introduction of LRI also in the quadratic term leads to similar results as we discuss below). Our numerical results are obtained using the 4th-order Yoshida symplectic scheme with time step such that the energy is conserved within 4 to 5 significant digits. The class of initial configurations we have chosen is of the “water-bag” type, *i.e.*, zero positions and momenta drawn randomly from a uniform distribution.

Let us begin our study with a systematic investigation of the *largest Lyapunov exponent*  $\lambda$  characterising the ergodicity of the dynamics for different values of  $\alpha$ ,  $N$  and specific energies  $u = U(N)/N$  (unless otherwise stated, we consider  $\alpha_{lin} \rightarrow \infty$ ). In fig. 1 we have plotted  $\lambda$  *vs.* the system size  $N$  for different  $\alpha$  values, ranging from 0 to 10. The critical value  $\alpha = 1$ , as was also found in [11], clearly distinguishes between the following two distinct regimes:

- i) For  $\alpha \geq 1$  the Lyapunov exponent  $\lambda$  tends to stabilise at a finite and positive value as  $N$  increases.
- ii) For  $\alpha < 1$  the largest Lyapunov exponents are observed to *decrease* with system size as  $N^{-\kappa(\alpha)}$ , where the dependence of the exponent  $\kappa(\alpha)$  on  $\alpha$  is shown in the inset of fig. 1.

A remark is in order here concerning the behaviour of  $\lambda$  as  $N \rightarrow \infty$ . As is evident in fig. 1, especially in the case  $\alpha = 0$ , it is possible that as  $N$  becomes arbitrarily large,  $\lambda$  converges to a small (positive) value. This would imply that the system remains chaotic in that limit. The accuracy of our results to date, however, does not permit us to distinguish between that case and  $\lambda = 0$  in the  $N \rightarrow \infty$  limit.

Based on the above (and on many other results available to date [9]), we expect that the system with short-range

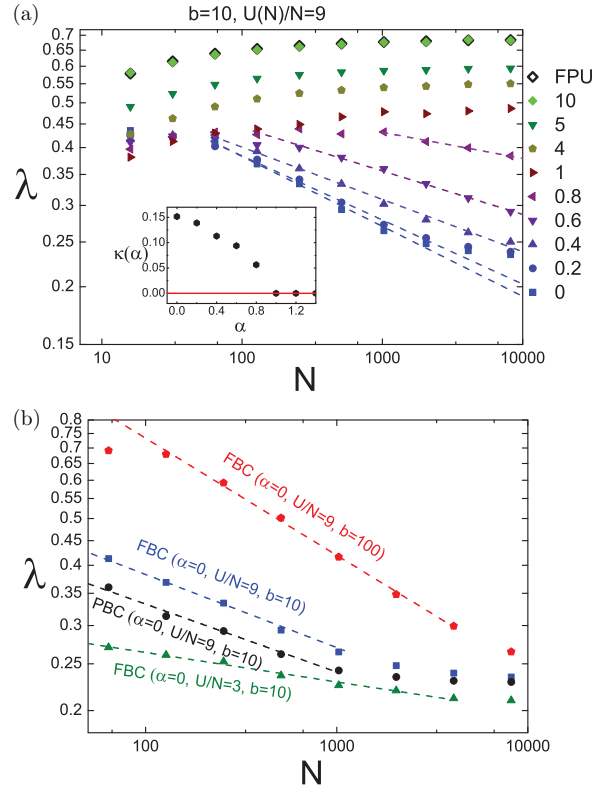


Fig. 1: (Colour on-line) Maximal Lyapunov exponent for increasing  $N$  calculated at  $t = 10^6$ . (a) For various  $\alpha$  values with  $U(N)/N = 9$ ,  $b = 10$  and FBC. (b) For various  $U(N)/N$ ,  $b$  values with  $\alpha = 0$  and both FBC, PBC.

interactions tends to a Boltzmann-Gibbs (BG) type of equilibrium in the thermodynamic limit, characterised by “strong” chaos. On the other hand, the case of LRI is expected to be “weakly” chaotic.

In order to check some of the expectations along the lines of nonextensive statistical mechanics (based on the nonadditive  $q$ -entropy) [14–17] and of the  $q$ -generalised Central Limit Theorem [18], we implement a molecular-dynamical computation of momentum distributions resulting from time averages of a single water-bag-type initial condition of (1), calculated over the interval  $[t_{min}, t_{max}]$ , where  $t_{min}$  is such that the kinetic temperature  $T \equiv 2K(t)/N$  ( $K(t)$  being the total kinetic energy of the system) stabilises to a nearly constant value.

In particular, for each of the histograms of fig. 2, we assign to each  $p_i$  the number of times that the momenta fall in the  $i$ -th band, calculated repeatedly for integer multiples of time (*i.e.* every  $\tau = 1$  for  $N = 2048$ ,  $\tau = 2$  for  $N = 4096$ ,  $\tau = 4$  for  $N = 8192$  etc. so that we always compare the same amount of data). Figure 2 displays the momentum distributions for  $\alpha = 0.7$  and  $1.4$  for  $N = 8192$ . In the top panel two histograms are shown, one for the time interval  $[10^5, 5 \cdot 10^5]$  and one for  $[4 \cdot 10^5, 8 \cdot 10^5]$ , which are well fitted by the  $q$ -Gaussian pdf:

$$P(p) = P(0)[1 + \beta(q-1)(pP(0))^2]^{1/(1-q)}, \quad q \geq 1, \quad (3)$$

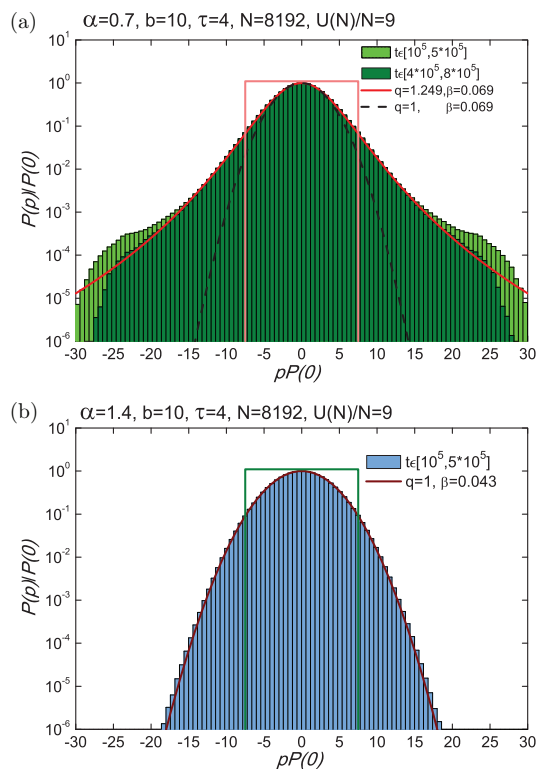


Fig. 2: (Colour on-line) Time-averaged momentum distributions for the system with  $N = 8192$ . (a)  $\alpha = 0.7$  for two different time intervals: The pdf seems to approach a  $q$ -Gaussian. (b)  $\alpha = 1.4$  and the distribution quickly approaches a Gaussian.

with  $q = 1.249$ . This value of  $q$  is nearly constant until  $t = 1.8 \cdot 10^6$ . For longer times  $q$  is observed to decrease as a power law in time and tends to the value 1, which explains why we call this a quasi-stationary state (QSS) [19]. In fig. 2(b) on the other hand the distribution follows from the beginning a pure Gaussian pdf ( $q \rightarrow 1$  in (3)) with  $\beta = 0.043$ .

The  $q$ -dependence on  $\alpha$  is shown in fig. 3, where the transition from  $q$ -statistics to BG statistics is evident as  $\alpha$  exceeds 1. Starting around  $q \simeq 1.33$ ,  $q$  reaches 1 at  $\alpha = 1.4$  for  $N = 16384$  particles calculated during the time interval  $[5 \cdot 10^5, 9 \cdot 10^5]$ . The data of fig. 3 is averaged over several realisations.

To check the robustness of our results with respect to  $q$ -statistics, we have computed the  $q$ -generalised kurtosis (referred to as  $q$ -kurtosis in [12,20]) defined as follows:

$$\kappa_q(q) = \frac{\int_{-\infty}^{\infty} dp p^4 [P(p)]^{2q-1} / \int_{-\infty}^{\infty} dp [P(p)]^{2q-1}}{3 \left[ \int_{-\infty}^{\infty} dp p^2 [P(p)]^q / \int_{-\infty}^{\infty} dp [P(p)]^q \right]^2}. \quad (4)$$

Using the  $q$  values found in fig. 3 we plot in fig. 4 the numerical data of  $q$ -kurtosis *vs.*  $q$  and find that it compares very well with the analytical curve  $\kappa_q(q) = (3-q)/(1+q)$  obtained by substituting the  $q$ -Gaussian pdf (3) in eq. (4).

Repeating the above study of the momenta distributions for the case where LRI are introduced *only* in the

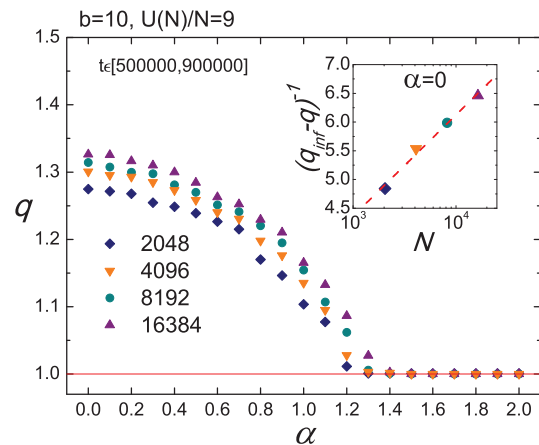


Fig. 3: (Colour on-line)  $\alpha$ -dependence of the index  $q$  for  $b = 10$  and  $U(N)/N = 9$  averaged over 4 independent realisations when  $N$  is 2048, 4096, 8192 and 2 realisations for  $N = 16384$ , all taken in the time interval  $t \in [5 \cdot 10^5, 9 \cdot 10^5]$ . Inset:  $(q_\infty - q)^{-1}$  *vs.*  $N$ , for the data of the main figure with  $\alpha = 0$ ;  $q_\infty$  has a value estimated around 1.48, and is the intercept of the linear dependence of  $q$  on  $1/\log N$ . The fitting line shown is  $(q_\infty - q)^{-1} = 1.76 \log N - 0.9$ .

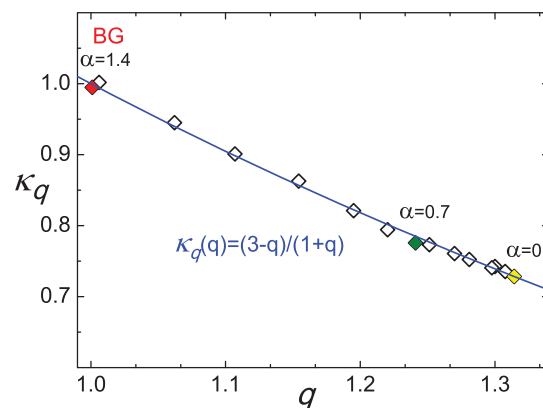


Fig. 4: (Colour on-line)  $q$ -dependence of the  $q$ -kurtosis  $\kappa_q$  for typical values of  $\alpha$ , together with the analytical prediction  $\kappa_q = (3-q)/(1+q)$  (blue curve) for the data of fig. 3 which corresponds to  $N = 8192$ .

quadratic part of the potential of the FPU  $\beta$ -model, *i.e.* for  $\alpha \rightarrow \infty$ , we find significant differences. First of all the phonon band shrinks with  $\alpha_{lin}$ , until it collapses onto a single value when  $\alpha_{lin}$  vanishes. For random initial conditions and a large variety of values for  $b$  and for  $U(N)/N$ , the time averaged momentum distributions are *all purely Gaussian*, as in fig. 5(a). Therefore, we conclude that  $q$ -Gaussian statistics occurs when *nonlinear* LRI are present and completely disappear in the presence of purely linear LRI. On the other hand, when both linear and nonlinear LRI apply in the FPU model, acting with two different ranges of interaction,  $\alpha_{lin}$  and  $\alpha$ , respectively, the value of  $q$  remains unchanged independently of the linear range, as can be seen in fig. 5(b).

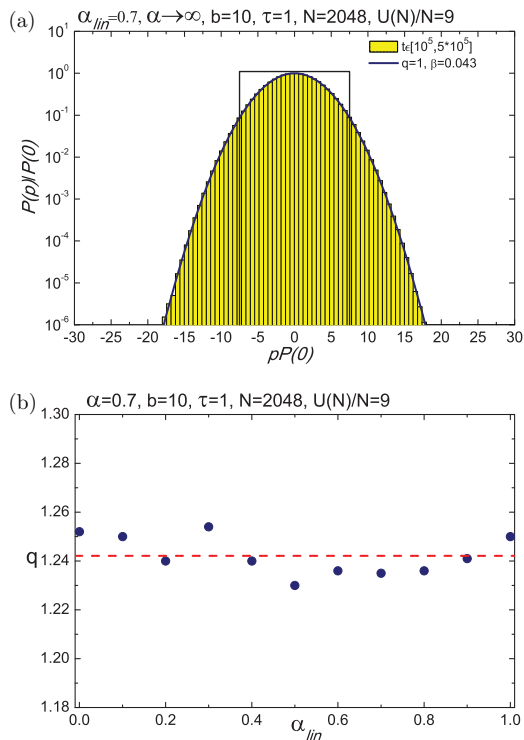


Fig. 5: (Colour on-line) (a) Time-averaged momentum distribution for linear LRI. (b)  $q$  values for the mixed system: the linear range of interaction  $\alpha_{lin}$  is a running parameter, while the nonlinear range is fixed at  $\alpha = 0.7$ .

Several papers have neatly shown the spontaneous emergence of  $q$ -Gaussians in the mean-field model of coupled planar rotators [12,13]. Their appearance is evidently due to the higher-order terms in the potential  $V = \sum_{i,j} \frac{1 - \cos(\vartheta_i - \vartheta_j)}{r_{i,j}^\alpha}$ , beyond the quadratic ones, the first being of the quartic type as in our FPU  $\beta$ -model. Thus, we conjecture that such phenomena appear in virtually any nonlinear nonintegrable lattice of the form

$$\mathcal{H} = \frac{1}{2} \sum_i p_i^2 + \sum_{i,j} V(x_i - x_j)/|i - j|^\alpha. \quad (5)$$

In the rest of the paper we study a fundamental question concerning the time evolution of  $q$ . For this purpose it is enough to restrict to the case of nonlinear LRI of Hamiltonian (1). As can be seen in fig. 6,  $q$  can decrease slowly in time, and eventually might reach the value  $q = 1$ . The  $q$ -logarithm of the distributions *vs.* the squared momenta appears as a straight line with slope  $-\beta$  only when the value of  $q$  is the appropriate one, as shown in fig. 6. The red dashed line represents a least squares fitting in the regime  $[0, 350]$ . Two sizes  $N = 4096$  and  $N = 16384$  have been considered at the times  $8 \cdot 10^5$ ,  $1.6 \cdot 10^6$  and  $4 \cdot 10^6$  in which the  $q$  values are accurately determined. However, the whole picture is quite subtle. Indeed, fig. 7(b) displays an interesting crossover between two regimes in the form of a “phase diagram”, which, for each fixed  $b$ , follows a straight line fit (in the  $1/N$ -*vs.*- $1/t_c^\gamma$  plane) of the

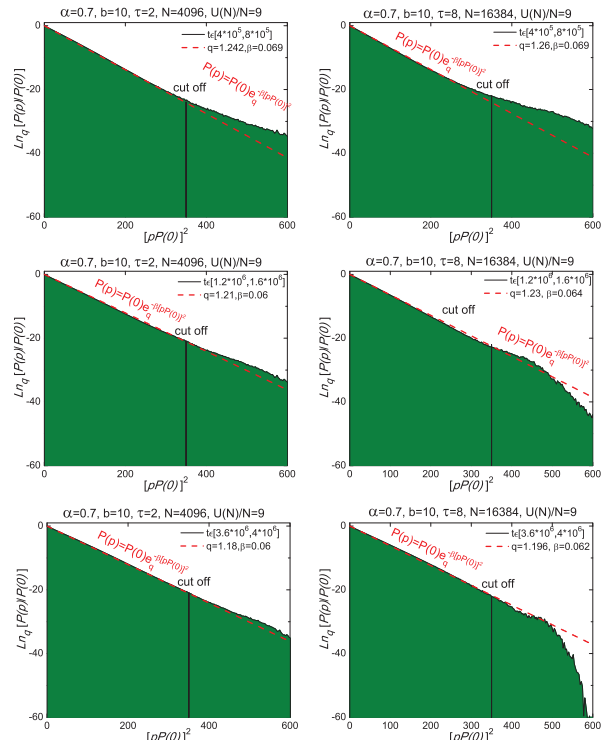


Fig. 6: (Colour on-line)  $q$ -Logarithm of the histogram *vs.* momenta squared. The dashed lines are the fittings  $P(p) = P(0)e^{-\beta(pP(0))^2}$  for appropriate  $q$  and  $\beta$  values ( $\alpha = 0.7$ ,  $b = 10$ ,  $U(N)/N = 9$ ). Left column:  $N = 4096$ . Right column:  $N = 16384$ . In these plots we can appreciate the robustness of the  $q$ -Gaussian form while time and  $N$  vary. In fact, the validity region where  $q$ -Gaussians are observed neatly improves with increasing  $N$ , as long as time adequately increases as well, consistently with what is shown in fig. 8.

data  $N \propto t^\gamma$ , separating the two “phases” (notice that, when we decrease the nonlinearity to  $b = 2$ , the slope of the frontier between the two phases decreases). Each point in the graph corresponds to a value of  $t = t_c$  representing the maximum time up to which  $q$  remains nearly constant; after this time,  $q$  starts (following a power law (see fig. 7(a))) approaching the BG value  $q = 1$ .

In fact, as we show in fig. 8, the crossover frontier can be represented for all  $b$  by a single straight line given approximately by

$$\frac{1}{N} \sim D(\alpha, u) \frac{b^{\delta(\alpha)}}{t_c^{\gamma(\alpha)}}, \quad (6)$$

where  $D \geq 0$  depends on  $\alpha$  and on the energy per particle  $u \equiv U(N)/N$ ; for  $\alpha = 0.7$ ,  $\delta \simeq 0.27$  and  $\gamma \simeq 1.36$ . For  $\alpha > 1$ , of course,  $D$  vanishes and the system is expected to be uniformly ergodic, following BG statistics. For  $\alpha < 1$  on the other hand, all available numerical evidence strongly suggests that the system follows  $q$ -statistics during a possibly non-ergodic QSS of “weak chaos”, as if it were trapped (for large but finite  $N$ ) in a subspace of the full phase space, where it lives as a QSS for a very long time.

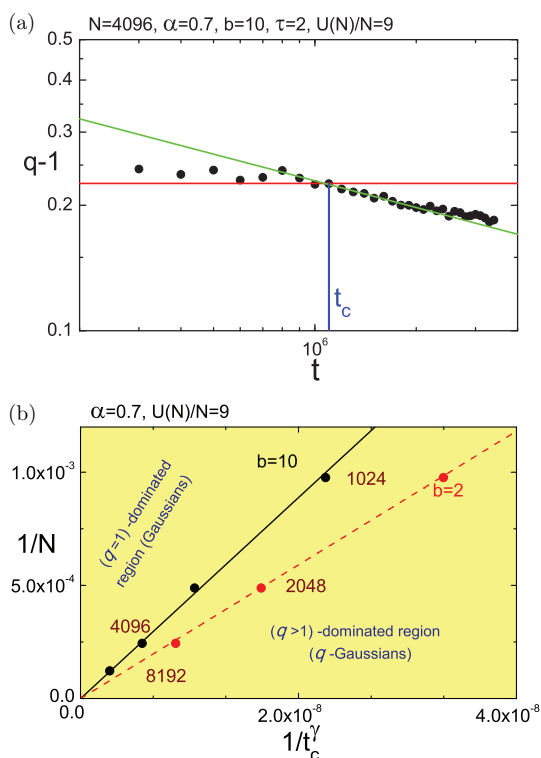


Fig. 7: (Colour on-line) (a) Evolution of  $q-1$  in double logarithmic scale also for  $u \equiv U(N)/N = 9$ . Each point corresponds to 4 realisations of a time average in a running window of width  $w = 2 \cdot 10^5$ .  $N$  is 4096 and the  $t_c$  is defined as the intersection between the two lines. For fixed  $N$ , the QSS exists for times up to  $t_c$ , and the system slowly relaxes towards a BG behaviour for times above  $t_c$ . (b) Crossover frontier between the Gaussian and  $q$ -Gaussian thermostatical regions for the system sizes  $N = 1024, 2048, 4096, 8192$  at specific energy  $u = 9$ , calculated for two cases,  $b = 2$  and  $b = 10$ . The fitting lines are  $1/N = 4.44 \cdot 10^4 / t_c^\gamma$  and  $1/N = 2.95 \cdot 10^4 / t_c^\gamma$  with  $\gamma = 1.365$ .

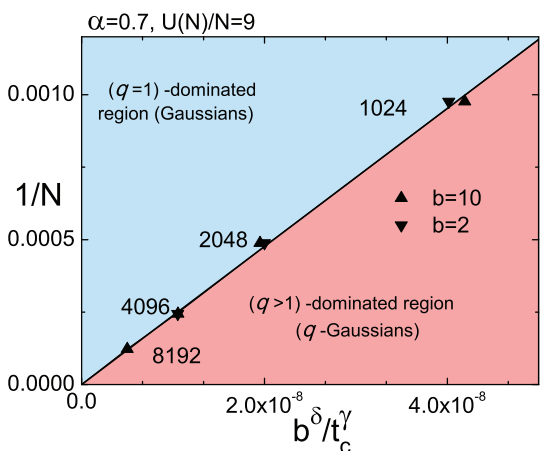


Fig. 8: (Colour on-line) A unified overview of the crossover frontier of fig. 7(b), combining the  $b$  values. The fitting straight line is  $1/N = Db^\delta / t_c^\gamma$ , with  $D = 2.3818 \times 10^4$ ,  $\delta = 0.27048$ , and  $\gamma = 1.365$ .

As a final summarising remark, we emphasise the nonuniformity, for *long-range interactions* (i.e.,  $\alpha$  small enough), of the  $(N, t) \rightarrow (\infty, \infty)$  limit implied by the diagram of fig. 8. Clearly, in the  $\lim_{N \rightarrow \infty} \lim_{t \rightarrow \infty}$  ordering it is the  $q = 1$  behaviour that prevails, while in the  $\lim_{t \rightarrow \infty} \lim_{N \rightarrow \infty}$  ordering it is the  $q > 1$  statistics that becomes dominant. These results have been obtained from dynamical first principles (Newton's law), *without any a priori hypothesis* about entropy or whatever similar thermodynamical quantities.

\*\*\*

We acknowledge very fruitful remarks by L. J. L. CIRTO. HC is grateful to Prof. R. QUISPEL and the Mathematics Department of La Trobe University for their hospitality, during October–December, 2013, where part of the work reported here was carried out. One of us (CT) gratefully acknowledges partial financial support by the Brazilian Agencies CNPq, Faperj and Capes. All of us acknowledge that this research has been co-financed by the European Union (European Social Fund-ESF) and Greek national funds through the Operational Program “Education and Lifelong Learning” of the National Strategic Reference Framework (NSRF) - Research Funding Program: *Thales. Investing in knowledge society through the European Social Fund.*

## REFERENCES

- [1] GIBBS J. W., *Elementary Principles in Statistical Mechanics - Developed with Especial Reference to the Rational Foundation of Thermodynamics* (C. Scribner's Sons, New York, 1902; Yale University Press, New Haven, 1948; OX Bow Press, Woodbridge, Conn., 1981).
- [2] ANTONI M. and RUFFO S., *Phys. Rev. E*, **52** (1995) 2361.
- [3] FLACH S., *Phys. Rev. E*, **58** (1998) R4116.
- [4] DAUXOIS T., LATORA V., RAPISARDA A., RUFFO S. and TORCINI A., in *Lect. Notes Phys.*, edited by DAUXOIS T., RUFFO S., ARIMONDO E. and WILKENS M., Vol. **602** (Springer) 2002, p. 458.
- [5] TARASOV V. E. and ZASLAVSKY G. M., *Commun. Nonlinear Sci. Numer. Simul.*, **11** (2006) 885.
- [6] FERMI E., PASTA J. and ULAM S., Los Alamos, Report No. LA-1940 (1955); NEWELL A. C., *Nonlinear Wave Motion, Lect. Appl. Math.*, Vol. **15** (AMS, Providence) 1974, pp. 143–155; BERMAN G. P. and IZRAILEV F. M., *Chaos*, **15** (2005) 015104.
- [7] LEPRI S., LIVI R. and POLITI A., *Phys. Rep.*, **377** (2003) 1; *Chaos*, **15** (2005) 015118.
- [8] BENETTIN G., LIVI R. and PONNO A., *J. Stat. Phys.*, **135** (2009) 873; CARATI A., *AIP Conf. Proc.*, **965** (2007) 43.
- [9] ANTONOPOULOS CH. and BOUNTIS T., *Phys. Rev. E*, **73** (2006) 056206; CHRISTODOULIDI H., EFTHYMIPOULOS C. and BOUNTIS T., *Phys. Rev. E*, **81** (2010) 016210; ANTONOPOULOS CH. and CHRISTODOULIDI H., *Int. J. Bifurcat. Chaos*, **21** (2011) 2285; BOUNTIS T. and SKOKOS H., *Complex Hamiltonian Dynamics, Springer Series in Synergetics* (Springer-Verlag, Berlin) 2012.

- [10] LEO M., LEO R. A. and TEMPESTA P., *J. Stat. Mech.* (2010) P04021; LEO M., LEO R. A., TEMPESTA P. and TSALLIS C., *Phys. Rev. E*, **85** (2012) 031149; LEO M., LEO R. A. and TEMPESTA P., *Ann. Phys. (N.Y.)*, **333** (2013) 12.
- [11] ANTENEODO C. and TSALLIS C., *Phys. Rev. Lett.*, **80** (1998) 5313.
- [12] CIRTO L. J. L., ASSIS V. and TSALLIS C., *Physica A*, **393** (2013) 286.
- [13] PLUCHINO A., RAPISARDA A. and TSALLIS C., *EPL*, **80** (2007) 26002; *EPL*, **83** (2008) 30011.
- [14] TSALLIS C., *Stat. Phys.*, **52** (1988) 479 (First appeared as preprint in 1987: CBPF-NF-062/87, ISSN 0029-3865, Centro Brasileiro de Pesquisas Fisicas, Rio de Janeiro).
- [15] GELL-MANN M. and TSALLIS C. (Editors), *Nonextensive Entropy - Interdisciplinary Applications* (Oxford University Press, New York) 2004.
- [16] TSALLIS C., *Introduction to Nonextensive Statistical Mechanics - Approaching a Complex World* (Springer, New York) 2009.
- [17] TSALLIS C., *Contemp. Phys.*, **55** (2014) 179.
- [18] UMAROV S., TSALLIS C. and STEINBERG S., *Milan J. Math.*, **76** (2008) 307; UMAROV S., TSALLIS C., GELL-MANN M. and STEINBERG S., *J. Math. Phys.*, **51** (2010) 033502; HAHN M. G., JIANG X. X. and UMAROV S., *J. Phys. A*, **43** (2010) 165208; HILHORST H. J., *J. Stat. Mech.* (2010) P10023; JAUREGUI M., TSALLIS C. and CURADO E. M. F., *J. Stat. Mech.* (2011) P10016; JAUREGUI M. and TSALLIS C., *Phys. Lett. A*, **375** (2011) 2085; PLASTINO A. and ROCCA M. C., *Milan J. Math.*, **80** (2012) 243.
- [19] ANTONOPOULOS CH., BOUNTIS T. and BASIOS V., *Physica A*, **390** (2011) 3290.
- [20] TSALLIS C., PLASTINO A. R. and ALVAREZ-ESTRADA R. F., *J. Math. Phys.*, **50** (2009) 043303.